C. R. Geoscience 343 (2011) 397–405

Contents lists available at ScienceDirect

Comptes Rendus Geoscience

www.sciencedirect.com

Petrology, geochemistry (Isotopic geochemistry)

Biological control of internal pH in scleractinian corals: Implications on paleo-pH and paleo-temperature reconstructions

Contrôle biologique du pH interne chez les coraux scléractiniaires : implications sur les reconstructions des paléo-pH et paléo-températures

Claire Rollion-Bard *, Marc Chaussidon, Christian France-Lanord

CNRS-UPR 2300, centre de recherches pétrographiques et géochimiques, université de Lorraine, BP 20, 54500 Vandœuvre-lès-Nancy, France

ARTICLE INFO

Article history:
Received 24 February 2011
Accepted after revision 31 May 2011

Presented by Jean Aubouin

Keywords:
Coral
Stable isotopes
pH
Ion probe
Precipitation kinetics

ABSTRACT

Elemental ratios and isotopic compositions of scleractinian corals are often used as proxies for the pH and the temperature of seawater from which they calcified. Nevertheless, these ratios recorded in the coral skeleton are offset from the ratios expected for equilibrium, due to vital effects. Ion microprobe $\delta^{11}B$ measurements were performed in a modern tropical coral, *Porites lutea*, and in a Mediterranean coral, *Cladocora caespitosa*, grown under two different pCO_2. We show that the $\delta^{11}B$ variations measured at micrometer scale are principally controlled by biology via modification of the pH near the calcification sites. The range of calculated pH allows to reproduce the range of $\delta^{18}O$ measured in corals via a kinetic model of oxygen isotopic equilibrium between water and DIC. Thus we show that temperature does not seem to be the primary control of the $\delta^{18}O$ variations in coral, though the constants of reaction and the isotopic fractionation values obviously depend on temperature.

Mots clés :
Corail
Isotopes stables
pH
Sonde ionique
Cinétique de précipitation

RÉSUMÉ

Les compositions élémentaires et isotopiques des coraux scléractiniaires sont souvent utilisées comme traceur des conditions environnementales dans lesquelles ils ont calcifié. Néanmoins, ces compositions chimiques ou isotopiques sont souvent différentes de celles attendues pour l'équilibre, cette différence étant attribuée aux effets vitaux. Des mesures de $\delta^{11}B$ par sonde ionique ont été réalisées dans un corail tropical moderne, *Porites lutea*, et dans un corail méditerranéen, *Cladocora caespitosa*, poussé sous deux conditions de pCO_2. Nous montrons que les variations mesurées sont principalement dues à la biologie via la modification du pH près des sites de calcification. La gamme de pH calculée nous permet de reproduire la gamme de $\delta^{18}O$ mesurée dans le corail *P. lutea* par le biais d'un modèle cinétique d'équilibre isotopique d'oxygène entre l'eau et le CID. Ainsi, nous montrons que la température ne semble pas être le facteur déterminant des variations de $\delta^{18}O$ dans les coraux, même si les constantes d'équilibre et les fractionnements isotopiques dépendent, eux, de la température.

1. Introduction

Coral skeletons are widely used as recorders of paleo-environmental conditions (for a review: Corrège, 2006;

* Corresponding author.
E-mail address: rollion@crpg.cnrs-nancy.fr (C. Rollion-Bard).

1631-0713/$ – see front matter © 2011 Académie des sciences. Published by Elsevier Masson SAS. All rights reserved.
doi:10.1016/j.crte.2011.05.003

Druffel, 1997). The isotopic composition of oxygen ($\delta^{18}O$) and trace element ratios are thought to vary with temperature (Mitsugushi et al., 1996; Weber and Woodhead, 1972) and thus provide indications of past seawater temperature. These reconstructions are based on empirical calibrations between a proxy (e.g. $\delta^{18}O$) and measured temperature. However, these isotopic compositions and element/Ca ratios differ from the equilibrium values determined for inorganic aragonite (Grossman and Ku, 1986), i.e. due to the so-called vital effects (Urey et al., 1951). Three main geochemical models are proposed to explain the oxygen isotope composition shift in coral skeletons: (1) pH variations in the fluid of calcification, which modifies the proportion of dissolved carbonate species (Adkins et al., 2003); (2) kinetic processes (McConnaughey, 2003; Sinclair and Risk, 2006), in which precipitation occurs before isotopic equilibrium between DIC and water; and (3) Rayleigh fractionation, in which the fluid of calcification is considered as a closed system (Cohen et al., 2006; Gagnon et al., 2007).

From in situ $\delta^{18}O$ measurements in scleractinian corals, large variations were documented (Allison et al., 2010b; Blamart et al., 2005; Juillet-Leclerc et al., 2009; Rollion-Bard and Erez, 2010; Rollion-Bard et al., 2003). These observations demonstrate that the vital effect observed in bulk samples mimics the average of micro-scale elemental and isotopic variability in the different parts of the skeleton (Allison et al., 2010a,b; Cohen et al., 2006; Meibom et al., 2003; Rollion-Bard et al., 2003; Sinclair, 2005). Indeed, we have already shown (Rollion-Bard et al., 2003) that pH can control the $\delta^{18}O$ values in corals via a change: (1) of the relative fractions of dissolved carbonate species (Usdowski and Hoefs, 1993; Usdowski et al., 1991; Zeebe, 1999, 2007); and (2) of the kinetics of their isotopic equilibration with water before carbonate precipitation (Section 5). The first calculation of the pH from $\delta^{11}B$ data in Rollion-Bard et al. (2003) was based on the historical fractionation factor between the two dissolved species (Kakihana et al., 1977). Since 2000, this fractionation factor was revisited (for a review: Pagani et al., 2005), and, based on in situ boron isotope measurements in foraminifera, it has now been shown (Rollion-Bard and Erez, 2010) that this fractionation factor is closed to the value determined by Klochko et al. (2006) – i.e. $\alpha_{4-3} = 0.97352$.

Here we report a re-calculation of pH from $\delta^{11}B$ data in *Porites lutea* corals (Rollion-Bard et al., 2003) in light of the new fractionation factor between the two boron dissolved species, and new $\delta^{11}B$ and $\delta^{18}O$ measurements in the same coral sample. We also report $\delta^{11}B$ analyses in Mediterranean scleractinian coral, *Cladocora caespitosa*, grown experimentally under two different atmospheric pCO_2, and so in different constant pH in order to observe the variability of the internal pH under constant environmental conditions. This will be interpreted in terms of kinetics of precipitation and in terms of biological control of internal pH by the coral.

2. Samples

To test the influence of environmental parameters on the $\delta^{11}B$ variability recorded in the coral skeleton, some measurements were performed on natural sample, *P. lutea*, and two corals, *C. caespitosa*, grown under constant laboratory conditions.

The *P. lutea* sample is a fragment of a modern massive coral collected at the Boulari Reef in New Caledonia in 1994 (166°26'26"E, 22°29'22"S, 5.6 m water depth, mean annual T = 23.15 °C, mean salinity S = 35.75 p.s.u., $\delta^{18}O_{sw} = 0.46‰$). Just after the collection, the sample was dried under the sun, and most of the organic matter was removed by water-jet. It was then cleaned by immersion in an ultrasonic bath in double distilled water, and dried. *C. caespitosa* is endemic of the Mediterranean Sea (Zibrowius, 1980). Two colonies were collected in the Bay of Villefranche (43°41'N, 7°18'E) at ≈25 m water depth in September 2006. An experiment was set up using two independent aquaria with two different pCO_2: ambient pCO_2 (i.e. 400 μatm, leading to a solution pH of 8.07) and elevated pCO_2 (≈700 μatm, leading to a solution pH of 7.86). The design of the experiments is already described in Rollion-Bard et al. (2009) and in more details in Rodolfo-Metalpa et al. (2010).

Briefly, ambient and elevated pCO_2 were obtained by bubbling ambient air and pure pCO_2 in two tanks. These conditions were maintained for 1 year. The tanks were continuously filled with Mediterranean seawater pumped from the bay of Villefranche (10 m depth) and then overflowed into the experimental aquaria. Corals were fed two times per week with some Artemia. The temperature, irradiance, and photoperiod were gradually changed in each aquarium in order to mimic the natural changes that occurred at the bay of Villefranche at *ca.* 20 m depth. At this depth, seawater temperature varied from 13 to 22 °C. pH was measured every 2 days using a Metrohm 862 pH mobile and an Orion electrode. Parameters of the carbonate system (pCO_2, CO_3^{2-}, HCO_3^-, DIC, and the aragonite saturation Ω_a) were calculated from pH, alkalinity, temperature and salinity using the Seacarb program (Lavigne and Gattuso, 2010) with equations from DOE (1994), Frankignoulle (1994), Zeebe and Wolf-Gladrow (2001), and Dickson et al. (2007). At the beginning of the experiment, coral skeletons were stained with Alizarin, which was used as a chronological marker, and was used for measuring subsequent skeletal growth. The colonies were carefully cleaned, and tissues were removed by using of NaOH (1 M).

Parts of the *C. caespitosa* skeleton above the Alizarin mark were mounted in epoxy and polished with diamond paste down to 1 μm. *P. lutea* sample was also polished down to 1-μm diamond paste (without epoxy) prior the ion probe analyses, and then gold coated.

3. Methods

Boron and oxygen isotopic analyses were carried out with the Cameca IMS 1270 ion microprobe at CRPG-CNRS, Nancy, France. The analytical settings are described in Blamart et al. (2007) for boron isotope measurements, and in Rollion-Bard et al. (2007) for oxygen isotope analyses. The boron isotopes were measured during two sessions for *P. lutea*: one in March 2002, and the other one in July 2010, and in one session for *C. caespitosa*. In summary, for boron isotopic measurements, a primary mass-filtered

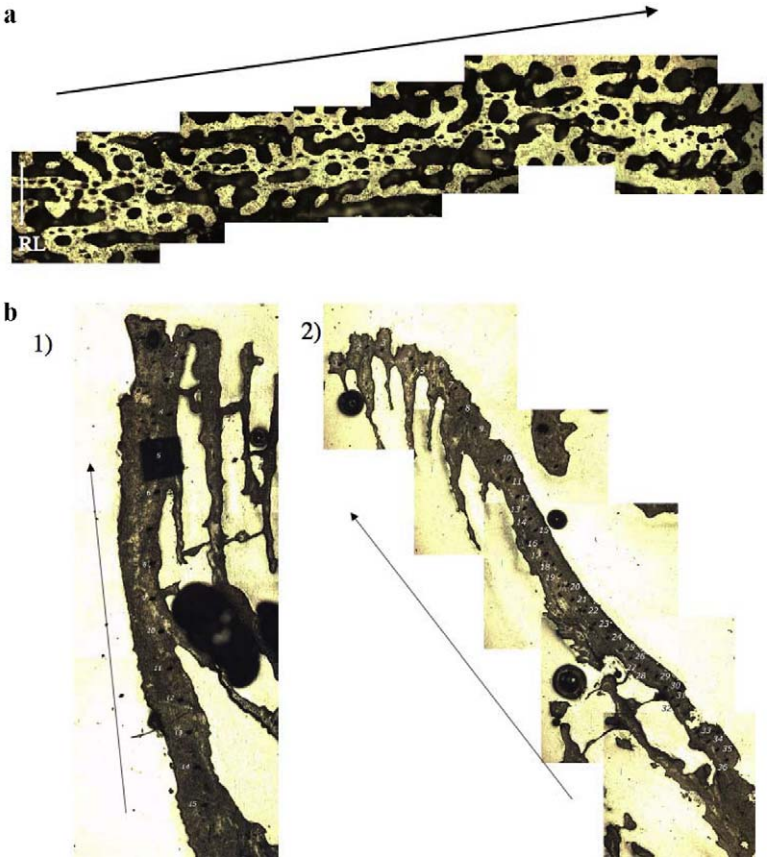

Fig. 1. a: reflected light picture of a gold-coated section of the *P. lutea* coral after SIMS analyses. Arrow indicates growth direction. RL: reference line; b: reflected light pictures of 2 transects of boron isotope analyses in *C. caespitosa*: (1) experiment at $pCO_2 \approx 400$ μatm, and (2) experiment at $pCO_2 \approx 700$ μatm. Arrows indicate maximum growth direction.

Fig. 1. a : photographie en lumière réfléchie de la section métallisée à l'or du corail *P. lutea* après les analyses à la microsonde ionique. La flèche indique le sens de croissance. RL : ligne de référence ; b : photographies en lumière réfléchie de la localisation des analyses des isotopes du bore dans *C. caespitosa* : (1) expérience à $pCO_2 \approx 400$ μatm, (2) expérience à $pCO_2 \approx 700$ μatm. Les flèches indiquent la direction de croissance maximale.

beam of $^{16}O^-$ ions with an intensity of 60–70 nA was focused into an aperture-delimited spot of approximately 15-μm wide and 30-μm long using Kohler illumination. The analyses were conducted in monocollection mode by peak jumping between the mass 9.5 (background), ^{10}B and ^{11}B. The reference material, WP 22, is an aragonite crystal with a B concentration of 22 ppm and a $\delta^{11}B$ value of 21‰. The internal error for $\delta^{11}B$ measurements was typically comprised between ±0.3 and 0.6‰ (1σ). Average external reproducibility, estimated from replicate measurements of the aragonite reference, was ±1.1‰ (1σ) for session 1, and ±0.8‰ (1σ) for session 2. These lead to typical total error (1σ) between ±0.9 and ±1.5‰ on $\delta^{11}B$ measurements.

For oxygen isotopic measurements, a primary beam of Cs^+ ions with an intensity of about 10 nA was focused into an aperture-delimited spot of approximately 15-μm wide and 30-μm long using Kohler illumination. Charge neutralization was achieved using the normal incidence electron gun. Measurements were conducted in multi-collection mode using two off-axis Faraday cups (L'2 and H1). All the $\delta^{18}O$ values are reported relative to the PDB standard. The reference materials are two calcite crystals (MEX and Carb) and one aragonite grain (Arg) with $\delta^{18}O_{PDB}$ of −7.05‰, −19.00‰, and −7.18‰, respectively. The internal error for $\delta^{18}O$ measurements was typically less than 0.1‰. Average external reproducibility, estimated from replicate measurements of the carbonate references, was ±0.4‰ (1σ).

All SIMS analyses were performed along the axis of maximum vertical coral growth, and also on trabeculae (vertical skeletal part) and synapticulae (horizontal skeletal part) for *P. lutea* (Fig. 1).

4. Results

4.1. P. lutea sample

Ion microprobe $\delta^{18}O$ measurements in *Porites* coral sample show large variation, from -10.6 ± 0.9‰ to -0.2 ± 0.5‰. This range of variation (≈10‰) cannot be ascribed to changes in environmental parameters since it would represent a temperature variation of about 50 °C (if we consider a temperature dependence of −0.2‰/°C, Epstein et al., 1953). The highest values are close to the isotopic equilibrium value for the aragonite-water system, using an average temperature of 23.15 °C, an average salinity of

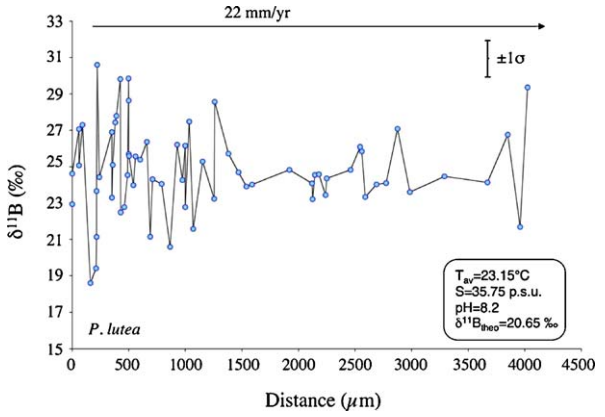

Fig. 2. *P. lutea* SIMS $\delta^{11}B$ measurements in function of distance (μm) relative to a fixed point (beginning of the profile). Considering a growth rate of about 22 mm/yr (Rollion-Bard et al., 2003), this profile covers between 2 and 3 months of coral growth.

Fig. 2. Mesures de $\delta^{11}B$ dans *P. lutea* par SIMS en fonction de la distance (en μm) par rapport à un point fixé correspondant au début du profil. En prenant un taux de croissance d'environ 22 mm/an (Rollion-Bard et al., 2003), la distance mesurée représente entre 2 et 3 mois de croissance du corail.

35.75 p.s.u., a $\delta^{18}O$ (in SMOW) of seawater of 0.46‰ and a pH of seawater of 8.2 (Grossman and Ku, 1986; Zeebe, 2007). Consequently the lowest values show a large and clear O-isotopic disequilibrium.

The $\delta^{11}B$ values show also a large variability, from 18.6 ± 1.5‰ to 30.6 ± 1.6‰ during session 1 (March 2002) and between 20.6 ± 0.8‰ and 29.84 ± 0.9‰ during session 2 (July 2010), showing then an overall variability of 12‰ (Fig. 2 and Table 1).

In this sample, it was not possible to distinguish the isotopic values of the centres of calcification (CoC) from the fibres, as the CoC are relatively small (less than 5 μm) compared to the ion probe spot (15 μm wide and 30 μm long). By consequence, the $\delta^{18}O$ and $\delta^{11}B$ values represent either a mixing of CoC and fibres signatures, or only fibres isotopic compositions, and all the values are then taken into account, even if it has been showed that it is unlikely that fibres and CoC derive from a single kinetic process in a common fluid of calcification (Rollion-Bard et al., 2010).

4.2. C. caespitosa samples

Despite the controlled pCO_2, leading to a constant pH, $\delta^{11}B$ values in each experiment show a large variability from 27.3 ± 0.7‰ to 32.3 ± 0.8 ‰, with an average $\delta^{11}B$ of 29.9 ± 1.3‰, for sample grown at pCO_2 of ≈400 μatm (i.e. pH = 8.07), and from 27.5 ± 0.7‰ to 31.2 ± 1.0‰, with an average $\delta^{11}B$ value of 29.3 ± 1.3‰, for sample grown at pCO_2 of ≈700 μatm (i.e. pH = 7.86) (Fig. 3). Both specimens show an overall range of ≈5‰, much smaller than in natural coral, *P. lutea*. Despite the large variability recorded in cultured *C. caespitosa* samples, the SIMS average $\delta^{11}B$ shows an increase with the surrounding pH, as expected from the relation between $\delta^{11}B$ in carbonates and pH of the solution and as shown from bulk coral measurements (Hönisch et al., 2004; Reynaud et al., 2004).

Table 1
Boron isotopic compositions measured in modern coral *Porites lutea*, and calculated pH from Eq. (1).

Tableau 1
Compositions isotopiques de bore, mesurées lors de deux sessions dans un corail moderne *Porites lutea* et pH calculés à partir de l'Éq. (1).

$\delta^{11}B$ (‰)	Error	pH
Session 1 (2002)		
22.93	1.36	8.42
27.06	1.40	8.68
27.30	1.43	8.70
21.14	1.43	8.29
23.66	1.47	8.46
30.59	1.39	8.92
24.43	1.58	8.51
19.41	1.38	8.15
27.43	1.44	8.71
25.10	1.56	8.56
29.80	1.40	8.87
22.77	1.59	8.40
24.53	1.52	8.52
25.58	1.53	8.59
28.64	1.65	8.79
22.49	1.38	8.39
23.29	1.51	8.44
18.61	1.53	8.08
25.07	1.47	8.56
24.62	1.53	8.53
Session 2 (2010)		
25.39	0.83	8.58
25.57	0.80	8.59
23.99	0.89	8.49
25.70	0.89	8.60
29.84	0.87	8.87
27.79	0.86	8.73
26.90	0.85	8.67
26.36	0.80	8.64
21.15	0.98	8.29
24.31	0.88	8.51
24.06	0.83	8.49
26.15	0.80	8.63
20.60	0.79	8.25
26.20	1.59	8.63
24.27	1.10	8.50
27.48	1.06	8.71
21.59	1.06	8.32
25.29	0.81	8.57
22.77	0.86	8.40
23.23	0.76	8.44
28.57	0.86	8.78
25.72	0.79	8.60
24.69	0.81	8.53
23.91	0.82	8.48
24.02	0.77	8.49
24.83	0.89	8.54
25.85	0.95	8.61
24.83	0.88	8.54
24.08	0.78	8.49
23.21	0.81	8.43
24.58	0.81	8.52
24.35	0.79	8.51
23.44	0.89	8.45
24.54	0.83	8.52
26.08	0.83	8.62
23.33	0.80	8.44
24.03	0.85	8.49
24.10	0.92	8.49
27.08	0.93	8.69
23.60	0.85	8.46
24.46	0.82	8.52
24.14	0.82	8.50
26.75	0.76	8.66
21.69	1.02	8.33
29.36	0.78	8.84

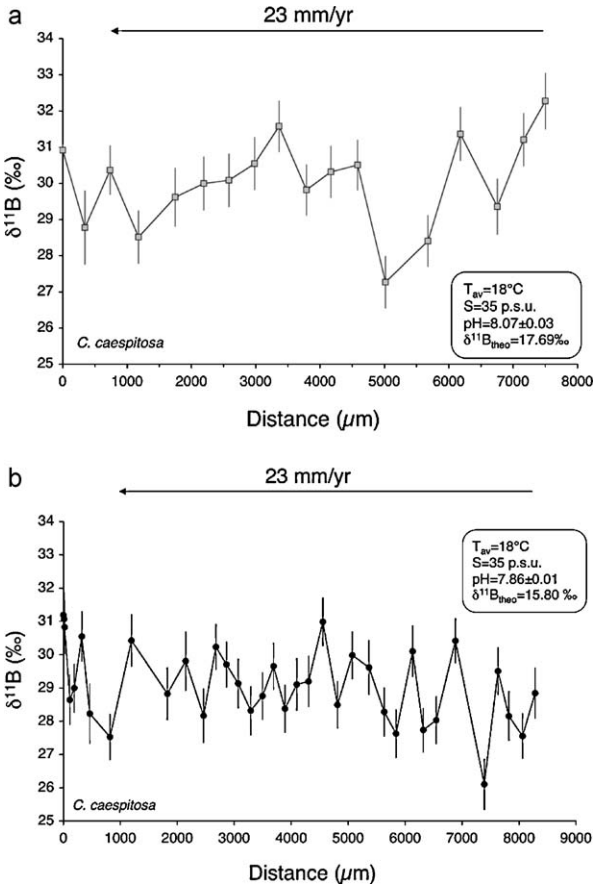

Fig. 3. SIMS $\delta^{11}B$ measurements in *C. caespitosa* samples. a: experiment at $pCO_2 \approx 400$ μatm; b: experiment at $pCO_2 \approx 700$ μatm. $\delta^{11}B_{theo}$ represents the $\delta^{11}B$ value of $B(OH)_4^-$ considering $\delta^{11}B_{sw} = 39.6‰$, T = 18 °C and S = 35 p.s.u. Arrows indicate maximum growth direction. Growth rate of 23 mm/yr was determined from an average calcification rate from Rodolfo-Metalpa et al. (2010).

Fig. 3. Mesures de $\delta^{11}B$ dans *C. caespitosa* par SIMS. a : expérience à $pCO_2 \approx 400$ μatm ; b : expérience à $pCO_2 \approx 700$ μatm. $\delta^{11}B_{theo}$ représente la valeur de $\delta^{11}B$ de $B(OH)_4^-$ en considérant $\delta^{11}B_{sw} = 39{,}6$ ‰, T = 18 °C et S = 35 p.s.u. Les flèches indiquent la direction de croissance maximale. Le taux de croissance de 23 mm/an a été calculé à partir d'un taux de calcification moyen à partir des données de Rodolfo-Metalpa et al. (2010).

We can also notice a difference of about 5‰ between *P. lutea* $\delta^{11}B$ values and those for *C. caespitosa*. This difference could be due to different total increase of the pH before the precipitation of the skeleton, and then resulting in different vital effects from species to species, as it was already observed in cultured corals (Pagani et al., 2005, for a review).

5. Discussion

5.1. Boron isotopes as seawater pH proxy?

In seawater, boron is present in the form of two dissolved species: boric acid $B(OH)_3$ and borate ion $B(OH)_4^-$. The proportion of these two dissolved species changes as a function of pH. Boron isotopes are fractionated between these two species, $B(OH)_3$ being enriched in ^{11}B by about 27.2‰ relative to $B(OH)_4^-$ (Klochko et al., 2006 determined at 25 °C and assuming no significant dependence with temperature over the considered range). The use of $\delta^{11}B$ of carbonates as pH proxy is in part based on the assumption that only $B(OH)_4^-$ is incorporated into carbonates (Hemming and Hanson, 1992; Hemming et al., 1995). Nevertheless, in recent studies (Klochko et al., 2009; Rollion-Bard et al., 2011), it was shown by NMR measurements that $B(OH)_3$ species could also be incorporated into biogenic carbonates. As the proportion of $B(OH)_3$ is not known in the coral species studied here, we chose to consider than only $B(OH)_4^-$is incorporated into the skeleton and then, the $\delta^{11}B$ of carbonates is pH-dependent according to:

$$pH = pK_B - \log\left(\frac{\delta^{11}B_{sw} - \delta^{11}B_c}{\alpha_{4-3}^{-1} \times \delta^{11}B_c - \delta^{11}B_{sw} + 1000 \times (\alpha_{4-3}^{-1} - 1)}\right) \quad (1)$$

where $\delta^{11}B_{sw}$ is the boron isotopic composition of seawater, $\delta^{11}B_c$ is the boron isotopic composition of the carbonate, pK_B is the dissociation constant between $B(OH)_3$ and $B(OH)_4^-$, and α_{4-3} is the fractionation factor between $B(OH)_3$ and $B(OH)_4^-$. In Eq. (1), $\delta^{11}B_{sw}$ is equal to 39.6‰ and is considered as constant for modern oceans (Foster et al., 2010), $\delta^{11}B_c$ is the value measured in the carbonate, pK_B has to be calculated as it is a function of temperature and salinity of the seawater (Dickson, 1990), and α_{4-3} is between 0.97352 and 0.975 (Klochko et al., 2006; Pagani et al., 2005). In the following, we use the fractionation factor of 0.97352 (Klochko et al., 2006).

Using Eq. (1), a pK_B of 8.61 (calculated with the average temperature and salinity at the sampling location from Dickson (1990) equation and the fractionation factor of Klochko et al. (2006), $\delta^{11}B$ data result in pH variations at the sites of calcification between 8.12 ± 0.1 and 8.94 ± 0.1. This pH range is smaller and more realistic than the previous one calculated in Rollion-Bard et al. (2003) (7.1 and 9.0). Moreover, it is very close to the pH range measured by microelectrodes in calicoblastic layers in the scleractinian coral *Galaxea fascicularis* (from 8.13 to 9.29, Al-Moghrabi et al., 2001).

5.2. Biological control of the internal pH

Large variations of the $\delta^{11}B$ data in both coral species are present in only a few micrometers (Figs. 2 and 3). Assuming a linear growth rate of about 2 cm/yr (Rollion-Bard et al., 2003), the $\delta^{11}B$ profile covers about 2–3 months of growth and so these variations occur in a very short timescale (less than 5 days, i.e. ≈200 μm). This heterogeneity in tropical corals has been previously reported for Sr/Ca (Cohen and Sohn, 2004; Meibom et al., 2003; Sinclair, 2005), Mg/Ca (Allison and Finch, 2007; Meibom et al., 2004; Sinclair, 2005), U/Ca (Sinclair, 2005), $\delta^{18}O$ (Adkins et al., 2003; Allison et al., 2010b; Rollion-Bard et al., 2003) and $\delta^{11}B$ (Allison et al., 2010a;

Rollion-Bard et al., 2003). No cyclical variation of the $\delta^{11}B$ signal seems present, contrary to what has been found for $\delta^{18}O$ (Rollion-Bard et al., 2003) and Sr/Ca (Meibom et al., 2003) in tropical corals. These variations are too large to be due to a change in environmental parameters (temperature, salinity, pH). It was also already shown that these variations in $\delta^{11}B$ seem to be not due to Rayleigh - evolution process (Rollion-Bard et al., 2010).

In the experimental samples (i.e. *C. caespitosa*), all the environmental parameters are kept constant (except the temperature, which varies between 13 °C and 22 °C): the corals grew under constant pH of the artificial seawater, i.e. for the experiment at $pCO_2 = 700$ μatm, the measured pH was in average 7.86 ± 0.01, and for the experiment at $pCO_2 = 400$ μatm, the average pH was 8.07 ± 0.03. If the coral $\delta^{11}B$ reflects directly seawater pH, then the expected $\delta^{11}B$ values would be respectively 15.80‰ at pH = 7.86 and 17.69‰ at pH = 8.07, using Eq. (1) with $\delta^{11}B$ of seawater at 39.6‰, $pK_B = 8.65$ (average T = 18 °C, S = 35 p.s.u), and fractionation factor of 0.97352. The measured $\delta^{11}B$ values are well above these theoretical values and indicate an elevated internal pH of 8.94 ± 0.09 (for $pCO_2 = 400$ μatm), and pH of 8.87 ± 0.08 (for $pCO_2 = 700$ μatm). These pH values calculated for the sites of calcification imply a strong control of the coral and that internal pH is mostly driven by biological processes, as it was already highlighted by $\delta^{11}B$ measurements in natural coral (Fig. 4). This pH increase at the sites of calcification relative to surrounding seawater is probably due to the removal of H^+ from the sites of calcification by the Ca^{2+}/H^+ ATPase (Dixon and Haynes, 1989; McConnaughey, 1989a; Niggli et al., 1982). It then results in the significant $CaCO_3$ supersaturation required to enhance carbonate precipitation.

5.3. Modelled effect of pH on kinetics of oxygen isotope equilibration between DIC and water

Calcification occurs via the reactions:

$$Ca^{2+} + HCO_3^- \Leftrightarrow CaCO_3 + H^+ \quad (1)$$

$$Ca^{2+} + CO_3^{2-} \Leftrightarrow CaCO_3 \quad (2)$$

$$CO_2 + H_2O \Leftrightarrow HCO_3^- + H^+ \text{ hydration} \quad (3)$$

$$CO_2 + OH^- \Leftrightarrow HCO_3^- \text{ hydroxylation} \quad (4)$$

All the reactions in the carbonate system are almost instantaneous, and only two reactions (reactions (3) and (4)) can constitute a limiting-step and have to be taken into account in order to calculate the rate of the isotopic equilibration between DIC and water. These two reactions are the production of HCO_3^- via reaction of CO_2 with either H_2O (hydration) or OH^- (hydroxylation).

Seawater has a $\delta^{18}O$ of −29.3‰ relative to PDB, whereas CO_2 in equilibrium with water has a $\delta^{18}O$ of about 10‰ (Kim and O'Neil, 1997). OH^- has a $\delta^{18}O$ value of about −67.3‰ (Usdowski and Hoefs, 1993). As a result of isotopic mass balance (2/3 of oxygen coming from CO_2, and 1/3 coming from H_2O or OH^-), HCO_3^- produced by hydration (reaction (3)) has an initial $\delta^{18}O_{PDB}$ of −3.2‰, whereas HCO_3^- produced by hydroxylation (reaction (4)) has an initial $\delta^{18}O_{PDB}$ of −15.8‰. The oxygen isotopic equilibrium of HCO_3^- value is 3.3‰.

For reactions (3) and (4), the equilibrium constants are calculated for the average temperature and salinity at the sampling location and a total DIC of 2000 μmol.kg^{-1} using

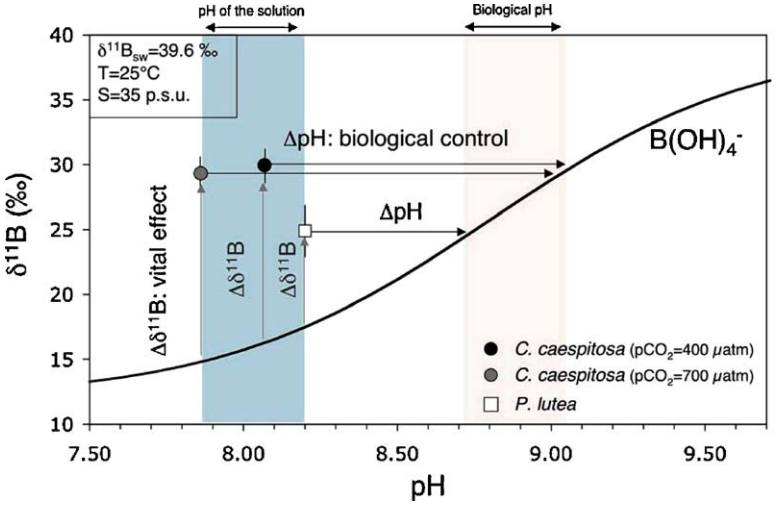

Fig. 4. Average $\delta^{11}B$ measured in corals versus pH of the solution. The vital effect is represented as the difference between the measured value and the theoretical value of $B(OH)_4^-$ (black curve), calculated for a seawater $\delta^{11}B$ of 39.6‰, temperature of 25 °C and salinity of 35 p.s.u. The biological control of the coral is indicated as the difference between the pH of the surrounding solution in which the coral grew and the pH near the sites of calcification (biological pH).

Fig. 4. $\delta^{11}B$ moyen mesuré dans les coraux en fonction du pH de la solution. L'effet vital est représenté par la différence entre la valeur mesurée et la valeur théorique de $B(OH)_4^-$ (courbe noire) calculée pour un $\delta^{11}B$ de l'eau de mer de 39,6 ‰, une température de 25 °C et une salinité de 35 p.s.u. Le contrôle biologique exercé par le corail est indiqué par la différence entre le pH de la solution dans laquelle ont poussé les coraux et le pH près des sites de calcification (pH biologique).

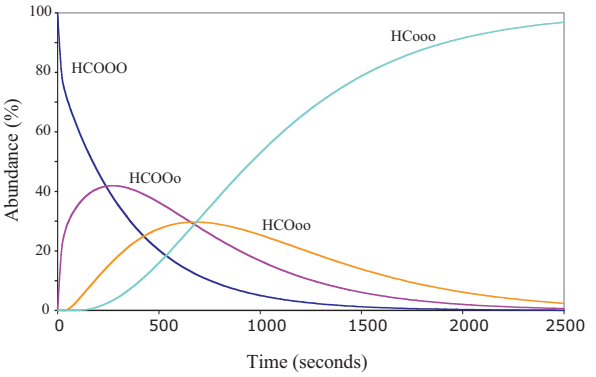

Fig. 5. Kinetics of the exchanges between HCO_3^- and H_2O calculated for a water with a pH of 7, temperature of 25 °C and salinity of 35 p.s.u. (DOE, 1994; Mehrbach et al., 1973; Millero and Pierrot, 1998; Zeebe and Wolf-Gladrow, 2001). The curves indicate the remaining fractions in the solution of the different species HCO_3^- having still 3 (HCOOO), 2 (HCOOo), 1 (HCOoo), and 0 (HCooo) atom(s) of oxygen initially present in HCO_3^-.

Fig. 5. Cinétique des échanges entre HCO_3^- et H_2O, calculée pour une eau à pH 7, une température de 25 °C et une salinité de 35 p.s.u. (DOE, 1994 ; Mehrbach et al., 1973 ; Millero et Pierrot, 1998 ; Zeebe et Wolf-Gladrow, 2001). Les courbes indiquent les fractions restantes dans la solution des espèces de HCO_3^- ayant encore trois (HCOOO), deux (HCOOo), un (HCOoo) et zéro (HCooo) atomes d'oxygène présents initialement dans HCO_3^-.

equations from Mehrbach et al. (1973), DOE (1994), Millero and Pierrot (1998), and Zeebe and Wolf-Gladrow (2001). The time required for HCO_3^- to reach oxygen isotopic equilibration with H_2O was then calculated according to McConnaughey (1989b) and Rollion-Bard et al. (2003), for several pH and for the reactions of hydration and hydroxylation (Fig. 5).

The proportion of HCO_3^- generated by hydration and hydroxylation is pH-dependent, hydroxylation being dominant for pH higher than 8.4 at 25 °C (Johnson, 1982). If we consider that isotopic equilibrium between $B(OH)_3$ and $B(OH)_4^-$ is almost instantaneous (Zeebe, 2005) and that the $\delta^{11}B$ signature of the carbonate is a proxy of pH at the site of calcification, in the pH range calculated, the fraction of HCO_3^- produced by hydration and hydroxylation are ≈67% and 33% respectively, at pH 8.1, and 24% and 76% at pH 8.9. Accordingly, the initial oxygen isotopic disequilibrium values for HCO_3^- would be −7.4‰ and −12.8‰ at pH 8.1 and 8.9, respectively. The $\delta^{18}O$ of the carbonate was calculated for different times and different pH values (Fig. 6) from the relative proportions of HCO_3^- and CO_3^{2-} in the solution and their $\delta^{18}O$, assuming that they are in isotopic equilibrium as their isotopic equilibration is quasi-instantaneous. H_2CO_3 is not taken into account as it is negligible for the range of pH considered here.

This calculation can predict the $\delta^{18}O$ of a carbonate for different pH and different time of equilibration between DIC and H_2O before the precipitation of the carbonate (Fig. 7). The isotopic equilibrium is reached in less than 12 h for pH smaller than 8.4. Almost half the $\delta^{18}O$ data measured by ion microprobe can be explained by residence times of less than 4 h (or more rapidly), considering no catalysis reactions; the rest would be precipitated more

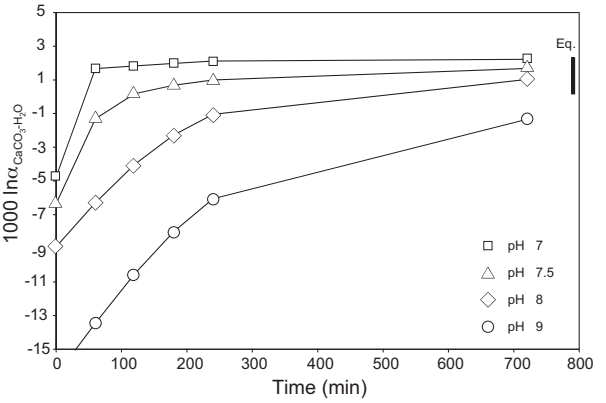

Fig. 6. Oxygen isotopic fractionation versus time calculated from the kinetics of the reactions of hydration and hydroxylation and from their proportion relative to the pH of the solution (Johnson, 1982) for a temperature of 25 °C, a salinity of 35 p.s.u., and pH of 7 (square), 7.5 (triangle), 8 (diamond), and 9 (circle). Eq. represents the range of equilibrium $\delta^{18}O$ for carbonates precipitated from seawater with pH between 7 and 9 (Usdowski and Hoefs, 1993; Zeebe, 1999, 2007).

Fig. 6. Fractionnement des isotopes de l'oxygène en fonction du temps calculé à partir des cinétiques de réaction d'hydratation et d'hydroxylation et de leur proportion selon le pH (Johnson, 1982) pour une température de 25 °C, une salinité de 35 p.s.u. et des pH de 7 (carré), 7,5 (triangle), 8 (losange) et 9 (cercle). Eq. représente la gamme de $\delta^{18}O$ pour des carbonates à l'équilibre avec une eau de mer entre les pH 7 et 9 (Usdowski et Hoefs, 1993 ; Zeebe, 1999, 2007).

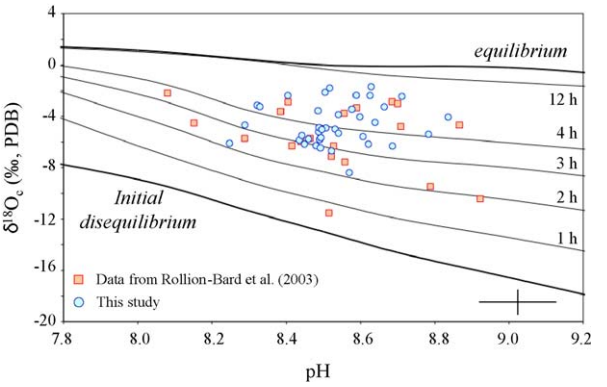

Fig. 7. *P. lutea* $\delta^{18}O$ measured by ion microprobe in function of pH calculated from measured $\delta^{11}B$ (square: Rollion-Bard et al., 2003; circle: this study). The lines represent the calculated evolution of carbonate $\delta^{18}O$ according to the pH of the solution for different time of equilibration of the carbonate species (essentially HCO_3^- and CO_3^{2-} at the pH considered) and water. Most of the measurements show that the necessary time for the precipitation of the carbonate constitutive of the coral skeleton would be between 2 and 3 h (without considering any catalysis). Error bars indicate the precision of each analysis (1 σ).

Fig. 7. $\delta^{18}O$ mesuré par sonde ionique en fonction des pH calculés à partir des $\delta^{11}B$ mesurés dans *P. lutea* (carré : Rollion-Bard et al., 2003 ; rond : cette étude). Les lignes représentent l'évolution calculée du $\delta^{18}O$ des carbonates selon le pH de la solution, pour différents temps d'équilibration des espèces carbonatées (essentiellement HCO_3^- et CO_3^{2-} aux pH considérés) et l'eau. La majorité des mesures montre que le temps nécessaire à la précipitation du carbonate constitutif du squelette corallien serait entre 2 et 3 heures (en ne considérant aucune catalyse). Les barres d'erreur indiquent la précision de chaque analyse (1 σ).

slowly. This difference in calcification rate could be explained by the significant variation of this rate between day and night, the daytime calcification being higher that the night-time one, the calcification being enhanced by the zooxanthellae (Chalker and Taylor, 1975; Goreau, 1959). This calcification is also different according to the structure of the coral (Clausen and Roth, 1975; Goreau, 1959), nevertheless, in this study, we do not see any evidence of relation with the coral architecture (i.e. synapticulae versus trabeculae).

6. Conclusions

The calculated internal pH is always higher than the pH of the surrounding seawater, which can only result from a strong biological control of the animal. The range of internal pH from $\delta^{11}B$ values for *P. lutea* tropical coral is between 8.1 and 8.9 ± 0.1, in agreement with direct pH measurements by micro-electrodes. Similarly, $\delta^{11}B$ measurements in cultured corals *C. caespitosa* imply a large range of internal pH (from 8.7 to 9.0). A better understanding of the link between pH of surrounding seawater and internal pH is required to improve significantly the use of $\delta^{11}B$ as paleo-pH proxy.

Combining $\delta^{11}B$ and $\delta^{18}O$ measurements in *P. lutea* sample, and a kinetic model of oxygen isotopic equilibrium between water and DIC, shows that half of the $\delta^{18}O$ data can be explained by residence time before the precipitation less than 4 h, the rest being explained by longer times of residence. However, these times of residence are probably too long relative to the typical times calculated from ^{45}Ca incorporation on the order of few minutes (Tambutté et al., 1995), as they do not take into account any catalysis processes (e.g. Ca-ATPase activity). Whatever the catalysis processes involved, the relation between internal pH and $\delta^{18}O$ variation is not modified. Even if the temperature controls the rate of reaction and the fractionation factor values, it appears as a second order parameter in the $\delta^{18}O$ variations in the coral.

Acknowledgments

We acknowledge the Region Lorraine for financial support. We thank S. Reynaud (Centre scientifique de Monaco) for providing *Cladocora caespitosa* samples. Two anonymous reviewers are thanked for their constructive comments and suggestions. This is CRPG contribution number 2120.

References

Adkins, J.F., Boyle, E.A., Curry, W.B., Lutringer, A., 2003. Stable isotopes in deep-sea corals and a new mechanism for "vital effect". Geochim. Cosmochim. Acta 67, 1129–1143.

Allison, N., Finch, A.A., 2007. High-temporal resolution Mg/Ca and Ba/Ca records in modern *Porites lobata* corals. Geochem. Geophys. Geosyst. 8, Q05001, doi:10.1029/2006GC001477.

Allison, N., Finch, A.A., EIMF, 2010a. $\delta^{11}B$, Sr, Mg and B in a modern Porites coral: the relationship between calcification site pH and skeletal chemistry. Geochim. Cosmochim. Acta 74, 1790–1800.

Allison, N., Finch, A.A., EIMF, 2010b. The potential origins and paleoenvironmental implications of high temporal resolution $\delta^{18}O$ heterogeneity in coral skeletons. Geochim. Cosmochim. Acta 74, 5537–5548.

Al-Moghrabi, S.M., Al-Horani, F.A., de Beer, D., 2001. Calcification by the scleractinian coral *Galaxea fascicularis*: direct measurements on calicoblastic layer using micro-sensors. In: 8th Int. Symp. on Biomineralization, 45.

Blamart, D., Rollion-Bard, C., Cuif, J.P., Juillet-Leclerc, A., Lutringer, A., van Weering, T.C.E., Henriet, J.P., 2005. C and O isotopes in a deep-sea coral (*Lophelia pertusa*) related to skeletal microstructure. In: Freiwald, A., Roberts, J.M. (Eds.), Cold-Water Corals, Ecosystems. Springer-Verlag, Berlin, pp. 1005–1020.

Blamart, Rollion-Bard, D., Meibom, A., Cuif, J.P., Juillet-Leclerc, A., Dauphin, Y., 2007. Correlation of boron isotopic composition with ultrastructure in the deep-sea coral *Lophelia pertusa*: implications for biomineralization and paleo-pH. Geochem. Geophys. Geosyst. 8, Q12001, doi:10.1029/2007GC001686.

Chalker, B.E., Taylor, D.L., 1975. Light-enhanced calcification and the role of oxidative phosphorylation in calcification of the coral *Acropora cerviconis*. Proc. R. Soc. Lond. B 190, 323–331.

Clausen, C.D., Roth, A.A., 1975. Estimation of coral growth-rates from laboratory ^{45}Ca-incorporation rates. Mar. Biol. 33, 85–91.

Cohen, A.L., Sohn, R.A., 2004. Tidal modulation of Sr/Ca ratios in Pacific reef coral. Geophys. Res. Lett. 31, L16310.

Cohen, A.L., Gaetini, G.A., Lundälv, T., Corliss, B.H., George, R.Y., 2006. Compositional variability in a cold-water scleractinian, *Lophelia pertusa*: New insights into "vital effects". Geochem. Geophys. Geosyst. 7, Q12004, doi:10.1029/2006GC001354.

Corrège, T., 2006. Sea surface temperature and salinity reconstruction from coral geochemical tracers. Palaeogeogr. Palaeoclimatol. Palaeoecol. 232, 408–428.

Dickson, A.G., 1990. Thermodynamics of the dissociation of boric acid in synthetic seawater from 273.15 to 318.15 K. Deep Sea Res. 37, 755–766.

Dickson, A.G., Sabine, C.L., Christian, J.R., 2007. Guide to best pratices for ocean CO_2 measurements. PICES Sp. Publi. 3, 1–191.

Dixon, D.A., Haynes, D.H., 1989. Ca^{2+} pumping ATPase of cardiac sarcolemma is insensitive to membrane potential produced by K^+ and Cl^- gradients but requires a source of counter-transportable H^+. J. Membr. Biol. 112, 169–183.

DOE, 1994. Handbook of methods for the analysis of the various parameters of the carbon dioxide system in the sea water; version 2. Dickson, A.G., Goyet, C. (Eds.), ORNL/CDIAC-74.

Druffel, E.R.M., 1997. Geochemistry of corals: proxies of past ocean chemistry, ocean circulation, and climate. Proc. Natl. Acad. Sci. U. S. A. 94, 8354–8361.

Epstein, S., Buchsbaum, H.A., Lowenstan, H.A., Urey, H.C., 1953. Revised carbonate-water isotopic temperature scale. Bull. Geol. Soc. Am. 64, 1315–1326.

Foster, G.L., Pogge van Strandman, P.A.E., Rae, J.W.B., 2010. Boron and magnesium isotopic composition of seawater. Geochem. Geophys. Geosyst. 11, Q08015, doi:10.1029/2010GC003201.

Frankignoulle, M., 1994. A complete set of buffer factors for acid/base CO_2 system in seawater. J. Mar. Syst. 5, 111–118.

Gagnon, A.C., Adkins, J.F., Fernandez, D.P., Robinson, L.F., 2007. Sr/Ca and Mg/Ca vital effects correlated with skeletal architecture in a scleractinian deep-sea coral and the role of Rayleigh fractionation. Earth Planet Sci. Lett. 261, 280–295.

Goreau, T.F., 1959. The physiology of skeleton formation in corals: I. A method for measuring the rate of calcium deposition by corals under different conditions. Biol. Bull. 116, 59–75.

Grossman, E.L., Ku, T.H., 1986. Oxygen and carbon isotope fractionation in biogenic aragonite: temperature effects. Chem. Geol. 59, 59–74.

Hemming, N.G., Hanson, G.N., 1992. Boron isotopic composition and concentration in modern marine carbonates. Geochim. Cosmochim. Acta 56, 537–543.

Hemming, N.G., Reeder, R.J., Hanson, G.N., 1995. Mineral-fluid partitioning and isotopic fractionation of boron in synthetic calcium carbonate. Geochim. Cosmochim. Acta 59, 371–379.

Hönisch, B., Hemming, N.G., Grottoli, A.G., Amat, A., Hanson, G.N., Bijma, J., 2004. Assessing scleractinian corals as recorders for paleo-pH: empirical calibration and vital effects. Geochim. Cosmochim. Acta 68, 3675–3685.

Johnson, K.S., 1982. Carbon dioxide hydration and dehydration kinetics in seawater. Limnol. Oceanogr. 27, 849–855.

Juillet-Leclerc, A., Reynaud, S., Rollion-Bard, C., Cuif, J.P., Dauphin, Y., Blamart, D., Ferrier-Pagès, C., Allemand, D., 2009. Oxygen isotopic signature of the skeletal microstructures in cultured corals: identification of vital effects. Geochim. Cosmochim. Acta 73, 5320–5332.

Kakihana, H., Kotaka, M., Satoh, S., Nomura, M., Okamoto, M., 1977. Fundamental studies on the ion-exchange of boron isotopes. Bull. Chem. Soc. Jpn 50, 158–163.

Kim, S.T., O'Neil, J.R., 1997. Equilibrium and nonequilibrium oxygen isotopes effects in synthetic carbonates. Geochim. Cosmochim. Acta 61, 3461–3475.

Klochko, K., Kaufman, A.J., Yao, W., Byrne, R.H., Tossell, J., 2006. Experimental measurements of boron isotopic fractionation in seawater. Earth Planet Sci. Lett. 248, 276–285.

Klochko, K., Cody, G.D., Tossell, J.A., Dera, P., Kaufman, A.J., 2009. Re-evaluating boron speciation in biogenic calcite and aragonite using ^{11}B MAS NMR. Geochim. Cosmochim. Acta 73, 1890–1900.

Lavigne, H., Gattuso, J.P., 2010. Seacarb: seawater carbonate chemistry with R. R package version 2.3.5. http://CRAN.R-project.org/package=seacarb.

McConnaughey, T.A., 1989a. ^{13}C and ^{18}O isotopic disequilibrium in biological carbonates: I. Patterns. Geochim. Cosmochim. Acta 53, 151–162.

McConnaughey, T.A., 1989b. ^{13}C and ^{18}O isotopic disequilibrium in biological carbonates: II. In vitro simulation of kinetic isotopic effects. Geochim. Cosmochim. Acta 53, 163–171.

McConnaughey, T.A., 2003. Sub-equilibrium oxygen-18 and carbon-13 levels in biological carbonates: carbonate and kinetic models. Coral Reefs 22, 316–327.

Mehrbach, C., Culberson, C.H., Hawley, J.E., Pytkowicz, R.M., 1973. Measurement of the apparent dissociation constant of carbonic acid in seawater at atmospheric pressure. Limnol. Oceanogr. 18, 897–907.

Meibom, A., Stage, M., Wooden, J., Constantz, B.R., Dunbar, R.B., Owen, A., Grumet, N., Bacon, C.R., Chamberlain, C.P., 2003. Monthly Strontium/Calcium oscillations in symbiotic coral aragonite: biological effects limiting the precision of the paleotemperature proxy. Geophys. Res. Lett. 30, 1418, doi:10.1029/2002GL016864.

Meibom, A., Cuif, J.-P., Hillion, F., Constantz, B.R., Juillet-Leclerc, A., Dauphin, Y., Watanabe, T., Dunbar, R.B., 2004. Distribution of magnesium in coral skeleton. Geophys. Res. Lett. 31, L23306, doi:10.1029/2004GL021313.

Millero, F.J., Pierrot, D., 1998. A chemical equilibrium model for natural waters. Aqua. Geochem. 4, 153–199.

Mitsugushi, T., Matsumoto, E., Abe, O., Uchida, T., Isdale, P.J., 1996. Mg/Ca thermometry in coral skeletons. Science 274, 961–963.

Niggli, V., Siegel, E., Carafoly, E., 1982. The purified Ca^{2+} pump of human erythrocyte memebranes catalyzes an electroneutral Ca^{2+}–H^{+} exchange in reconstituted liposomal systems. J. Biol. Chem. 257, 2350–2356.

Pagani, M., Lemarchand, D., Spivack, A., Gaillardet, J., 2005. A critical evaluation of the boron isotope-pH proxy: the accuracy of ancient ocean pH estimates. Geochim. Cosmochim. Acta 69, 953–961.

Reynaud, S., Hemming, G.N., Juillet-Leclerc, A., Gattuso, J.P., 2004. Effect of pCO_2 and temperature on the boron isotopic composition of the zooxanthellate coral Acropora sp. Coral Reefs 23, 539–546.

Rodolfo-Metalpa, R., Martin, S., Ferrier-Pagès, C., Gattuso, J.P., 2010. Response of the temperate coral *Cladocora caespitosa* to mid- and long-term exposure to pCO_2 and temperature levels projected for the year 2100 AD. Biogeosciences 7, 289–300.

Rollion-Bard, C., Erez, J., 2010. Intra-shell boron isotope ratios in the symbiont-bearing benthic foraminiferan *Amphistegina lobifera*: implications for δ^{11}B vital effects and paleo-pH reconstructions. Geochim. Cosmochim. Acta 74, 1530–1536.

Rollion-Bard, C., Chaussidon, M., France-Lanord, C., 2003. pH control on oxygen isotopic composition in symbiotic corals. Earth Planet. Sci. Lett. 215, 275–288.

Rollion-Bard, C., Mangin, D., Champenois, M., 2007. Development and application of oxygen and carbon isotopic measurements of biogenic carbonates by ion microprobe. Geostand. Geoanal. Res. 31, 39–50.

Rollion-Bard, C., Vigier, N., Meibom, A., Blamart, D., Reynaud, S., Rodolfo-Metalpa, R., Martin, S., Gattuso, J.P., 2009. Effect of environmental conditions and skeletal ultrastructure on the Li isotopic composition of scleractinian corals. Earth Planet. Sci. Lett. 286, 63–70.

Rollion-Bard, C., Blamart, D., Cuif, J.P., Dauphin, Y., 2010. *In situ* measurements of oxygen isotopic composition in deep-sea coral, *Lophelia pertusa*: re-examination of the current geochemical models of biomineralization. Geochim. Cosmochim. Acta 74, 1338–1349.

Rollion-Bard, C., Blamart, D., Trebosc, J., Tricot, G., Mussi, A., Cuif, J.-P., 2011. Boron isotopes as pH proxy: a new look at boron speciation in deep-sea corals using ^{11}B MAS NMR and EELS. Geochim. Cosmochim. Acta 75, 1003–1012.

Sinclair, D.J., 2005. Correlated trace element "vital effects" in tropical corals: a new geochemical tool for probing biomineralization. Geochim. Cosmochim. Acta 69, 3265–3284.

Sinclair, D.J., Risk, M.J., 2006. A numerical model of trace-element coprecipitation in a physicochemical calcification system: application to coral biomineralization and trace-element 'vital effects'. Geochim. Cosmochim. Acta 70, 3855–3868.

Tambutté, E., Allemand, D., Bourge, I., Gattuso, J.-P., Jaubert, J., 1995. An improved ^{45}Ca protocol for investigating physiological mechanisms in coral calcification. Mar. Biol. 122, 453–459.

Usdowski, E., Hoefs, J., 1993. Oxygen isotope exchange between carbonic acid, bicarbonate, carbonate, and water: a re-examination of the data of McCrea (1950) and an expression for the overall partitioning of oxygen isotopes between the carbonate species and water. Geochim. Cosmochim. Acta 57, 3815–3818.

Usdowski, E., Michaelis, J., Böttcher, M.E., Hoefs, J., 1991. Factors for the oxygen isotope equilibrium between aqueous and gaseous CO_2, carbonic acid, bicarbonate, carbonate, and water (19 °C). Z. Phys. Chem 170, 237–249.

Urey, H.C., Lowenstam, H.A., Epstein, S., McKinney, C.R., 1951. Measurements of paleotemperatures and temperatures of the Upper Cretaceous of England. Denmark, and the southeastern United States. Bull. Geol. Soc. Am. 62, 399–416.

Weber, J.N., Woodhead, P.M.J., 1972. Temperature dependence of oxygen-18 concentration in reef coral carbonates. J. Geophys. Res. 77, 463–473.

Zeebe, R.E., 1999. An explanation of the effect of seawater carbonate concentration on foraminiferal oxygen isotopes. Geochim. Cosmochim. Acta 63, 2001–2007.

Zeebe, R.E., 2005. Stable boron isotope fractionation between dissolved $B(OH)_3$ and $B(OH)_4^-$. Geochim. Cosmochim. Acta 69, 2753–2766.

Zeebe, R.E., 2007. An expression of the overall oxygen isotope fractionation between the sum of dissolved inorganic carbon and water. Geochem. Geophys. Geosyst. 8, Q09002, doi:10.1029/2007GC001663.

Zeebe, R.E., Wolf-Gladrow, D., 2001. CO_2 in seawater: equilibrium, kinetics, isotopes. Elsevier Oceanogr. 65, 346.

Zibrowius, H., 1980. Les scléractiniaires de Méditerranée et de l'Atlantique nord-oriental. Mem. Inst. Oceanogr. 11, 1–284.